

Article

Vibration Characteristics Control of Resonance Point in Vehicle: Fundamental Considerations of Control System without Displacement and Velocity Information

Keigo Ikeda ^{1,*}, Jumpei Kuroda ², Daigo Uchino ³, Kazuki Ogawa ³, Ayato Endo ⁴ , Taro Kato ⁵, Hideaki Kato ⁶  and Takayoshi Narita ⁶ 

¹ Department of Mechanical Engineering, Hokkaido University of Science, Sapporo 066-8585, Japan

² Course of Mechanical Engineering, Tokai University, Hiratsuka 259-1292, Japan

³ Course of Science and Technology, Tokai University, Hiratsuka 259-1292, Japan

⁴ Department of Electrical Engineering, Fukuoka Institute of Technology, Fukuoka 811-0295, Japan

⁵ Department of Mechanical Engineering, Tokyo University of Technology, Hachioji 192-0982, Japan

⁶ Department of Mechanical Systems Engineering, Tokai University, Hiratsuka 259-1292, Japan

* Correspondence: ikeda-k@hus.ac.jp; Tel.: +81-688-2296

Abstract: The deterioration of ride comfort in ultra-compact vehicles has recently become an increasing concern. Active seat suspension was proposed to improve the ride comfort of ultra-compact vehicles. An active seat suspension is a vibration control device that is easily installed. The general vibration control system of the active seat suspension is fed back to the displacement and velocity by integrating the measured seat acceleration. This control has problems, such as control delay and deviation by integration. In this study, we focused on vibration control using acceleration directly. First, we established a control model that feeds back the acceleration to terminate the error occurring in the integral process and investigated the change in vibration characteristics in the case where the feedback gain of acceleration was changed. Second, the control system was analyzed to investigate the performance of the control based on the frequency characteristics. As a result, it was confirmed that the frequency response changes when the feedback gain is changed. In acceleration feedback control, ride comfort was improved by selecting a proper feedback gain because the characteristics of frequency were changed by the gain.

Keywords: active seat suspension; ultra-compact vehicle; vibration control; ride comfort



Citation: Ikeda, K.; Kuroda, J.; Uchino, D.; Ogawa, K.; Endo, A.; Kato, T.; Kato, H.; Narita, T. Vibration Characteristics Control of Resonance Point in Vehicle: Fundamental Considerations of Control System without Displacement and Velocity Information. *Vibration* **2023**, *6*, 1–10. <https://doi.org/10.3390/vibration6010001>

Academic Editor: Jan Awrejcewicz

Received: 13 September 2022

Revised: 10 November 2022

Accepted: 23 December 2022

Published: 26 December 2022



Copyright: © 2022 by the authors. Licensee MDPI, Basel, Switzerland. This article is an open access article distributed under the terms and conditions of the Creative Commons Attribution (CC BY) license (<https://creativecommons.org/licenses/by/4.0/>).

1. Introduction

In recent years, ultracompact vehicles have been proposed as a new means of transportation for short distances. Ultra-compact vehicles are easy to drive and have high turning performance because of the very small body size, which seats one–two passengers. Therefore, vehicles are used in both urban and tourist areas. However, ultra-compact vehicles have a problem with ride comfort, owing to their simple internal structure. The ride comfort is particularly when driving on unpaved roads.

Oshinoya et al. proposed an “active seat suspension” system to improve the ride comfort of ultra-compact vehicles [1]. Active seat suspension is a vibration control device located in the seat area of a vehicle. Such systems can be easily installed.

An active seat suspension is a system in which the vibration of the seat is controlled using the detected acceleration of the seat surface. Magneto-viscous fluid, hydraulic, and servo actuators have been used for active seat suspension systems, but in ultra-compact vehicles, compact, lightweight, and high-thrust actuators are required in consideration of the operating environment. Therefore, we focused on voice coil motors to construct actuators with high thrust and response. We have proposed a masking method to change the ride quality using an activity seat suspension with a voice coil motor. Masking is

a method for reducing the impact of a disturbance input relative to the vibration input to the vehicle (disturbance) by applying a different frequency component to the active seat suspension (masker). The important factor is the amplitude of the masker vibration relative to that of the disturbance vibration. In other words, the thrust and stroke of the active seat suspension are very important, and we have confirmed the effectiveness of the proposed active seat suspension mechanism in improving ride comfort through masking [2]. In addition, we evaluated ride comfort using biometric information that can be measured continuously and in real time. We have proposed a control method that uses this biometric information to actively control the vibration input to the occupant according to their psychological state [3]. Furthermore, commonly devised seat suspensions have passive, semi-active, and active controls, and the control performance for each model varies widely [4–14]. Control methods such as robust control, fuzzy control, sliding mode control, adaptive control, and neural network control have been proposed for active seat suspension [15–22]. However, these control methods are state feedback control methods for displacement and velocity [23]. Generally, in ride quality evaluation, ISO 2631 and Janeway's ride quality limit curves are presented as frequency bands, and acceleration affects the ride quality [24,25]. Therefore, it is necessary to construct a control method that controls acceleration and designs acceleration that is comfortable for the occupant. In addition, each passenger has his or her own unique riding comfort and body shape as a result of vibration. It is necessary to provide ride comfort tailored to each individual occupant. For this reason, we have proposed a ride comfort control system tailored to each individual occupant, as shown in Figure 1. This system acquires the occupant's biometric information, predicts the occupant's psychological state from the biometric information, and controls the system according to the predicted psychological state. A method for predicting psychological states from biometric information has been reported [26], and this paper examines the control system. Based on the above system. We applied a feedback control algorithm that uses displacement and velocity calculated by integration of measured seat acceleration in the control system of an active seat suspension system [27]. However, control delay and deviation owing to the integral process can affect the control performance. Therefore, in this study, we focused on a vibration control system that directly feeds back acceleration. We investigated the frequency characteristics when the feedback gain was changed. Moreover, the control system was analyzed to investigate the control performance in the assumed case of an actual road environment.

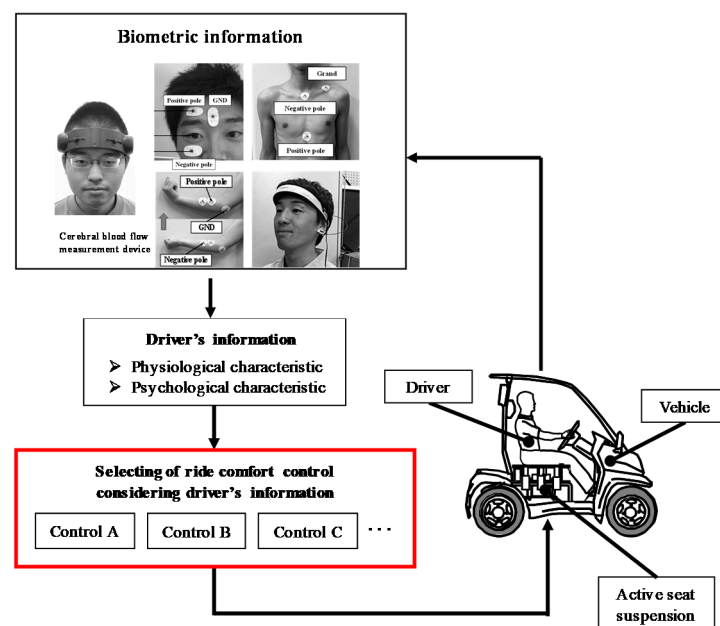


Figure 1. Ride comfort control system considering drivers.

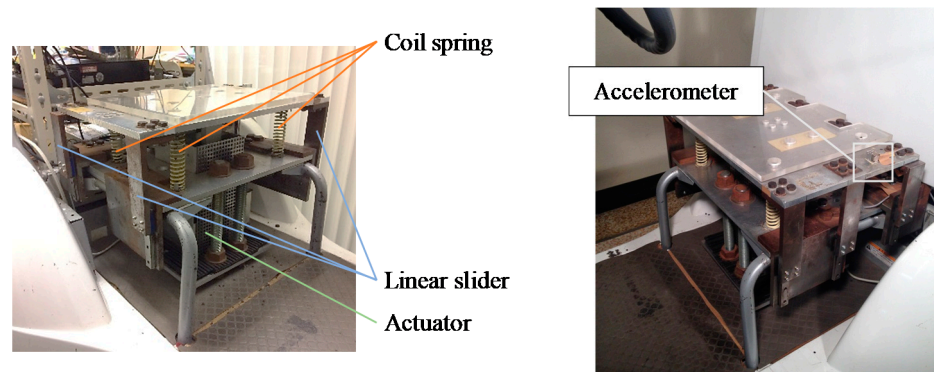
2. Active Seat Suspension

In this study, the control target was an active seat suspension system in an ultra-compact vehicle. Figure 2 shows an ultra-compact vehicle with active seat suspension. Figure 3 shows the active seat suspension and Figure 4 shows the control devices. An aluminum plate was used as the driver’s seat, which was supported by four coil springs and allowed to vibrate only in the vertical direction via a linear slider. A voice coil motor (VCM), which enables high-accuracy and high-speed control, was adopted for the control actuator and was located inside the active seat suspension, as shown in Figure 5. This provides the benefit of direct-drive maintenance-free control. Table 1 lists the specifications of the vehicle and VCM. The seat of the vehicle was controlled directly by the active seat suspension system, which was located under the seat. The controlled vibration was measured using an accelerometer mounted on the top of the seat. In previous studies, we conducted a driving experiment using an actual system and confirmed that the optimal control theory [28] and sliding mode control [29], which used velocity and displacement, were able to suppress the vibration of the seat. The investigation model of the active seat suspension in this study was the same as that used in previous studies [28,29].



Active seat suspension

Figure 2. Ultra-compact vehicle.



(a) Composition of active seat suspension

(b) Location of accelerometer

Figure 3. Active seat suspension.

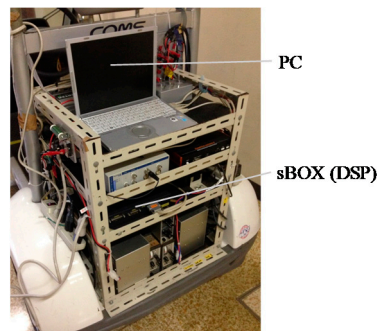


Figure 4. Control devices (back side of vehicle).

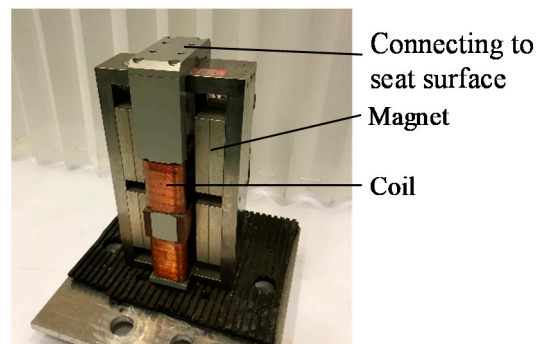


Figure 5. Voice coil motor.

Table 1. Specifications for the vehicle and VCM.

Ultra-Compact Vehicle: EVERYDAY COMS BASIC (Toyota Auto Body Co., Ltd.)	
Total weight [kg]	325
Length [mm]	1935
Whole width [mm]	955
Height [mm]	1600
Wheelbase [mm]	1280
Tread (front, rear) [mm]	840, 815
VCM (Aoyama Special Steel Co., Ltd.)	
Stroke [mm]	20
Thrust constant [N/A]	110
Nominal thrust [N]	160
Maximum thrust [N]	320
Rated current [A]	1.46

3. Modeling and Control System of Active Seat Suspension

The frequency characteristics and control performance of the acceleration feedback system were investigated using analysis software from Simulink The MathWorks, Inc. A mathematical model of the active seat suspension described in Section 2 was established. As shown in Section 2, the active seat suspension comprises coil springs, linear sliders, and actuators. Therefore, the active seat suspension was modeled as a one degree-of-freedom vibration system, as shown in Figure 6. In this study, we focused on vibration characteristics

without considering the characteristics of the electric circuit. The motion equation of the model is as follows:

$$m\ddot{y} + c(\dot{y} - \dot{z}) + k(y - z) = -f\ddot{y} \tag{1}$$

where m is the sum of the masses of the seat and driver including their legs; k is the spring constant (as the sum of the four springs); c is the apparent damping coefficient considering the friction of the linear slider, internal damping of the spring, and concomitant mechanical elements; f is the feedback gain for seat acceleration; y is the displacement of the seat; and z is the displacement of the floor-connected active seat suspension. The right-hand side shows the driving force of the voice-coil motor. This shows the direct feedback of acceleration.

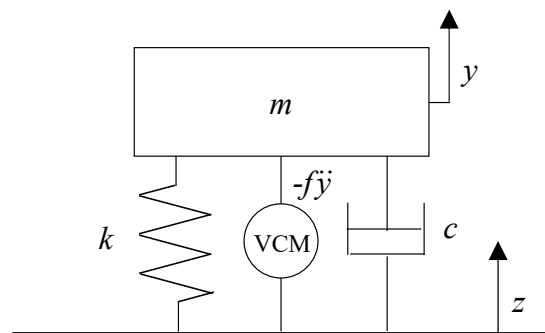


Figure 6. Model of active seat suspension.

4. Frequency Characteristics of Acceleration Feedback System

In this section, the characteristics of the acceleration feedback system were investigated using the model described in Section 3. In particular, the mass was changed virtually by the feedback of acceleration in the control system, as shown in Equation (1). It is conceivable that the frequency characteristics of the control system changed because the resonance point was moved by the proposed control. Therefore, from Equation (2) changes in the frequency characteristics by acceleration feedback control were investigated using simulations.

$$\omega = \sqrt{\frac{k}{m}} \tag{2}$$

m : mass k : spring coefficient

The vibration response of the active seat suspension was investigated using the model shown in Figure 7, when a sine wave disturbance z was input. Four values were used for the feedback gain ($f = -20, 0, 20, 40$). Here, $f = 0$ denotes the state without control. Table 2 lists the parameters of the vibration model used in this study. The frequency of the sine wave disturbance was varied from 1 Hz to 20 Hz. The peak-to-peak amplitude of the sine wave disturbance was 10 mm. Figure 8 shows the transmissibility of the vibration at a disturbance frequency of 1–20 Hz. Here, transmissibility of vibration was calculated by the ratio of the root mean square (RMS) of displacements y and z . When considering a one-degree-of-freedom vibration system, the vibration transfer coefficient is given by Equation (3). The vibration transfer coefficient has a value greater than 1 in the resonance region, and there is a vibration isolation region where the vibration transfer coefficient is less than 1 in the vibration frequency region sufficiently higher than the resonance. The natural frequency ratio ω/ω_n when the vibration transfer coefficient is 1 can be obtained as shown in Equation (7).

$$T = \left| \frac{U_0^x}{V_0} \right| = \sqrt{\frac{1 + 4\zeta^2(\omega/\omega_n)^2}{\{1 - (\omega/\omega_n)^2\}^2 + 4\zeta^2(\omega/\omega_n)^2}} \tag{3}$$

$$T = \sqrt{\frac{1 + 4\zeta(\omega/\omega_n)^2}{1 - 2(\omega/\omega_n)^2 + (\omega/\omega_n)^4 + 4\zeta^2(\omega/\omega_n)^2}} \tag{4}$$

$$- 2(\omega/\omega_n) + (\omega/\omega_n)^4 = 1 \tag{5}$$

$$(\omega/\omega_n)^2\{(\omega/\omega_n)^2 - 2\} = 0 \tag{6}$$

$$\omega/\omega_n = 0, \sqrt{2} \tag{7}$$

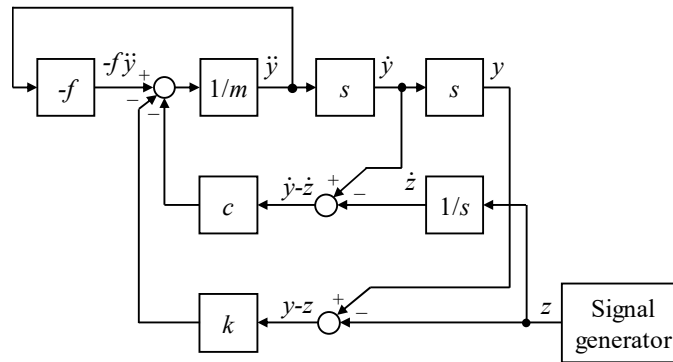


Figure 7. Simulation model.

Table 2. Specifications of simulation model.

Parameter	Value
Mass m [kg]	64
Damping c [Ns/m]	145
Spring k [N/m]	23,485
Feedback gain f [-]	-20, 0, 20, 40

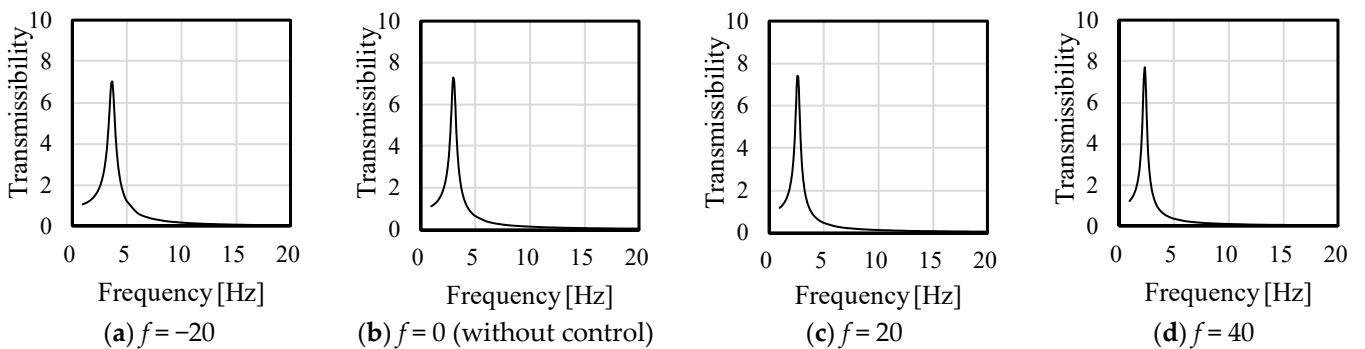


Figure 8. Transmissibility of each frequency of sine wave.

From the above, the range of vibration isolation is defined as the range of natural frequencies that is more than $\sqrt{2}$ times the natural frequency.

Each control model had resonance points at frequencies of 1–5 Hz, and the transmissibility was very low at frequencies greater than 5 Hz. Figure 9 shows an expanded section of Figure 8 from 1–5 Hz. The frequency of the resonance point was decreased by increasing the feedback gain, because the mass was virtually increased. Therefore, the area where transmissibility was less than 1.0 was wider. In the case of decreasing the feedback gain, the frequency of the resonance point was increased by virtually decreasing the mass. Table 3 lists the maximum values of the transmissibility and resonance frequency of the system. In the case of negative feedback gain, although the range where transmissibility was more than 1.0 became wider than the result without acceleration feedback, the maximum

transmissibility at the resonance point decreased. Therefore, in the proposed acceleration feedback system, there is a tradeoff between the maximum transmissibility at the resonance point and the range where the transmissibility is less than 1.0.

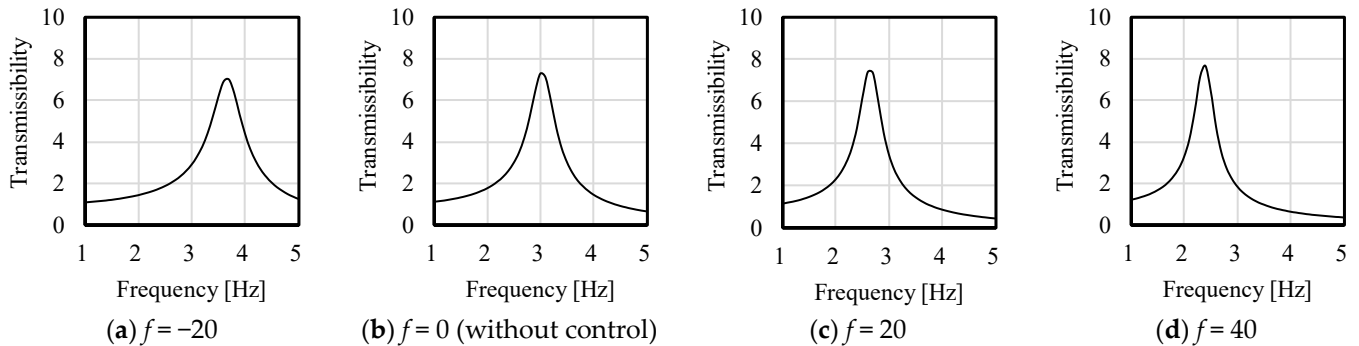


Figure 9. Transmissibility of each frequency of sine wave (1–5 Hz).

Table 3. Maximum transmissibility and that frequency.

Feedback Gain f	Frequency [Hz]	Transmissibility
-20	3.7	6.99
0 (without control)	3.0	7.27
20	2.6	7.39
40	2.4	7.68

5. Effect of Control Performance by Feedback Gain

It was confirmed that acceleration feedback could change the vibration characteristics of the active seat suspension system. However, the effect of acceleration feedback control on the control performance has not been clarified. Therefore, we performed a numerical simulation in the case of a disturbance input to an ultra-compact vehicle similar to an actual travelling situation and investigated the effect.

The simulation in this section used the same model as in Section 4. The disturbance was white noise filtered using a low-pass filter at 20 Hz, and the RMS of the disturbance was set to 5 mm. The feedback gain and parameters of the vibration model were the same as those described in Section 4. Figure 10 shows the time histories of (a) disturbance and (b–e) displacement, velocity, and acceleration of feedback gains -20, 0, 20, and 40. The frequency characteristics of the system were changed by the acceleration feedback compared to the conditions without control. Moreover, the amplitude was changed by control. Figure 11 shows the transmissibility from disturbance z to displacement y for each feedback condition. In the cases of $f = -20$ and 20, the vibration amplitude increased compared to the condition without control. However, the vibration was suppressed by acceleration feedback at $f = 40$. By setting the feedback gain to -20, the apparent mass changes, and the vibration is considered to be amplified because it is out of the vibration isolation range. When the feedback gain is set to 20, the vibration is within the vibration isolation range, but the vibration is amplified due to the large peak of vibration as shown in Chapter 3 (Figure 8). When the feedback gain is set to 40, the vibration isolation zone and the vibration peak are well balanced within the range of the present excitation conditions, and the vibration is considered to have been suppressed.

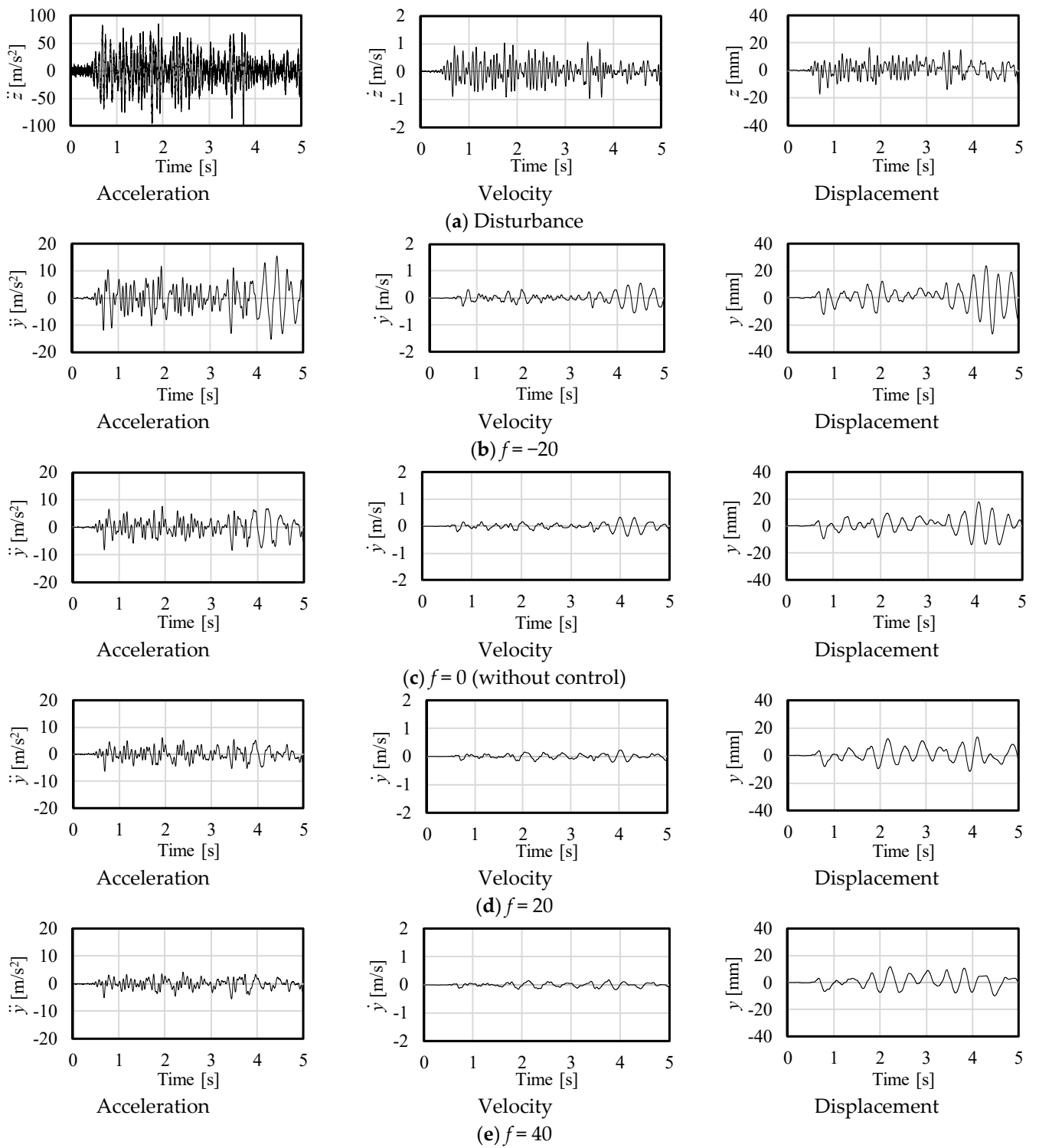


Figure 10. Time histories of vibration.

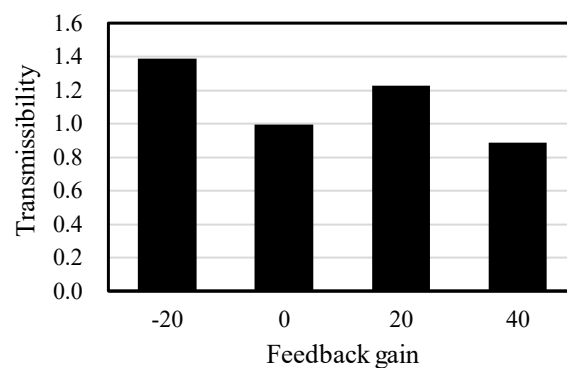


Figure 11. Control performance of each feedback system.

6. Conclusions

In this study, we established a control model that feeds back the acceleration to terminate the error occurring in the integral process and investigated the change in vibration characteristics in the case where the feedback gain of acceleration was changed. The simulation assumed that the actual driving conditions were satisfied, and the frequency characteristics were investigated. From these results, we conclude the following.

- i. Change of frequency characteristics affects control performance by change of resonance point.
- ii. It is possible to suppress vibrations by applying an appropriate feedback gain. In the future, we intend to perform experiments using an actual apparatus and establish a multi-degree-of-freedom vibration control system for an actual vehicle.

In the future, frequency characteristics will be confirmed with multiple occupants using actual equipment. Furthermore, a system that changes the acceleration gain of vibration in real time according to the psychological state of the occupants by combining biometric information will be constructed.

Author Contributions: K.I., summarized this study and wrote the manuscript. J.K., D.U. and K.O., carried out the experiment. A.E., T.K., H.K. and T.N., are experimental advisor for this experiment. All authors have read and agreed to the published version of the manuscript.

Funding: This research was funded by Japan Keirin Association (JKA) Foundation, grant number 2021M-129.

Data Availability Statement: Not applicable.

Conflicts of Interest: The authors declare no conflict of interest.

References

- Oshinoya, Y.; Arai, H.; Ishibashi, K. Experimental Study on Active Seat Suspension for a Small Vehicle. *Int. J. Appl. Math.* **2004**, *19*, 437–443. [[CrossRef](#)]
- Ikeda, K.; Endo, A.; Minowa, R.; Narita, T.; Kato, H. Ride Comfort Control System Considering Physiological and Psychological Characteristics: Effect of Masking on Vertical Vibration on Passengers. *MDPI Actuators* **2018**, *7*, 42–54. [[CrossRef](#)]
- Endo, A.; Ikeda, K.; Mashino, M.; Kato, H.; Narita, T. Ride comfort control system using driver's psychological state: Experimental consideration on heart rate variability. *Int. J. Appl. Math.* **2019**, *59*, 977–984. [[CrossRef](#)]
- Ning, D.; Sun, S.; Li, H.; Du, H.; Li, W. Active Control of an Innovative Seat Suspension System with Acceleration Measurement Based Friction Estimation. *J. Sound Vib.* **2016**, *384*, 28–44. [[CrossRef](#)]
- Ning, D.; Sun, S.; Zhang, F.; Du, H.; Li, W.; Zhang, B. Disturbance Observer Based Takagi-Sugeno Fuzzy Control for An Active Seat Suspension. *Mech. Syst. Signal Process.* **2017**, *93*, 515–530. [[CrossRef](#)]
- Schimmels, J.M. Improved Vibration Isolating Seat Suspension Designs Based on Position-Dependent Nonlinear Stiffness and Damping Characteristics. *J. Dyn. Syst. Meas.* **2003**, *125*, 330–338.
- Sever, M.; Yazici, H. Disturbance Observer Based Optimal Controller Design for Active Suspension Systems. *IFAC Pap.* **2016**, *49*, 105–110. [[CrossRef](#)]
- Sun, S.; Ning, D.; Yang, J.; Du, H.; Zhang, S.; Li, W. A seat Suspension with a Rotary Magnetorheological Damper for Heavy Duty Vehicles. *Smart Mater. Struct.* **2016**, *25*, 105032. [[CrossRef](#)]

9. Zhao, Y.; Sun, W.; Gao, H. Robust Control Synthesis for Seat Suspension Systems with Actuator Saturation and Time-Varying Input Delay. *J. Sound Vib.* **2010**, *329*, 4335–4353. [[CrossRef](#)]
10. Mahesh, S.L.; Pramod, D.; Shrivijay, B.P. Active Control of Uncertain Seat Suspension System Based on a State and Disturbance Observer. *IEEE Trans. Syst. Man Cybern. Syst.* **2020**, *50*, 840–850.
11. Tang, X.; Ning, D.; Du, H.; Li, W.; Wen, W. Takagi-Sugeno Fuzzy Model-Based Semi-Active Control for the Seat Suspension with An Electrorheological Damper. *IEEE Access* **2022**, *8*, 98027–98037. [[CrossRef](#)]
12. More, A.; Deshpande, A. A Multiple Sliding Surface Based Control for Active Seat Suspension System. In Proceedings of the 2021 5th International Conference on Intelligent Computing and Control Systems, Madurai, India, 6–8 May 2021.
13. Lie, L.; Li, X. Event-Triggered Tracking Control for Active Seat Suspension Systems with Time-Varying Full-State Constraints. *IEEE Trans. Syst. Man Cybern. Syst.* **2022**, *5*, 582–590. [[CrossRef](#)]
14. Taghavifar, H.; Rakheja, S. Multi-Objective Optimal Robust Seat Suspension Control of Off-Road Vehicles in the Presence of Disturbance and Parametric Uncertainty Using Metaheuristics. *IEEE Trans. Intell. Veh.* **2020**, *5*, 372–384. [[CrossRef](#)]
15. Oya, M.; Harada, H.; Araki, Y. An Active Suspension Controller Achieving the Best Ride Comfort at Any Specified Location on A Vehicle. *JSD* **2007**, *1*, 245–256. [[CrossRef](#)]
16. Jianmin, S.; Yi, S. A Fuzzy Method Improving Vehicle Ride Comfort and Road Holding Capability. In Proceedings of the 2007 2nd IEEE Conference on Industrial Electronics and Applications, Harbin, China, 23–25 May 2007.
17. Choi, H.D.; Ahn, C.K.; Shi, P.; Wu, L.; Lim, M.T. Dynamic output-feedback dissipative control for T-S fuzzy systems with time-varying input delay and output constraints. *IEEE Trans. Fuzzy Syst.* **2017**, *25*, 511–526. [[CrossRef](#)]
18. Taghavifar, H.; Mardani, A.; Hu, C.; Qin, Y. Adaptive Robust Nonlinear Active Suspension Control Using an Observer-Based Modified Sliding Mode Interval μ -2 Fuzzy Neural Network. *IEEE Trans. Intell. Veh.* **2020**, *5*, 53–62. [[CrossRef](#)]
19. Rath, J.J.; Defoort, M.; Karimi, H.R.; Veluvolu, K.C. Output Feedback Active Suspension Control with Higher Order Terminal Sliding Mode. *IEEE Trans. Ind. Electron.* **2016**, *64*, 1392–1403. [[CrossRef](#)]
20. Pan, H.; Jing, X.; Sun, W.; Gao, H. A Bioinspired Dynamics-Based Adaptive Tracking Control for Nonlinear Suspension Systems. *IEEE Trans. Control. Syst. Technol.* **2017**, *26*, 903–914. [[CrossRef](#)]
21. Pan, H.; Sun, W.; Jing, X.; Gao, H.; Yao, J. Adaptive Tracking Control for Active Suspension Systems with Non-Ideal Actuators. *J. Sound Vib.* **2017**, *399*, 2–20. [[CrossRef](#)]
22. Zhao, F.; Ge, S.S.; Tu, F.; Qin, Y.; Dong, M. Adaptive Neural Network Control for Active Suspension System with Actuator Saturation. *IET Control. Theory A* **2016**, *10*, 1696–1705. [[CrossRef](#)]
23. Wenxing, L.; Haipineg, D.; Donghong, N.; Weihua, L. Robust Adaptive Sliding mode PI control for active vehicle seat suspension systems. In Proceedings of the 2019 Chinese Control and Decision Conference (CCDC), Nanchang, China, 3–5 June 2019.
24. ISO 2631 1978; Guide for the Evaluation of Human Exposure to Whole-Body Vibration. International Organization for Standardization: Geneva, Switzerland, 1978.
25. Janeway, R.N. Vehicle vibration limit to fit the passenger. *SAE J.* **1948**, 56.
26. Ikeda, K.; Kuroda, J.; Uchino, D.; Ogawa, K.; Endo, A.; Kato, T.; Kato, H.; Narita, T. A Study of a Ride Comfort Control System for Ultra-Compact Vehicles Using Biometric Information. *Appl. Sci.* **2022**, *12*, 7425. [[CrossRef](#)]
27. Oshinoya, Y.; Ishibashi, K.; Arai, H. Basic Examination of Improvement on Riding Comfort with An Active Seat Suspension of A Small Electric Vehicle. *J. Jpn. Soc. Appl. Electromagn. Mech.* **2013**, *11*, 209–215. (In Japanese)
28. Mashino, M.; Ishida, M.; Narita, T.; Kato, H.; Yamamoto, Y. Active Seat Suspension for Ultra-Compact Electric Vehicle (Fundamental Consideration on Electrooculogram When Fall from the Bump). *Int. Symp. Appl. Electromagn. Mech.* **2016**, *52*, 215–222. [[CrossRef](#)]
29. Kato, H.; Hasegawa, S.; Oshinoya, Y. Active Control of Ultra-Compact Vehicle Seat with Voice Coil Motor (Examination of the Control Performances during Driving on a Bad Road). *J. Magn. Soc. Jpn.* **2013**, *37*, 95–101. [[CrossRef](#)]

Disclaimer/Publisher’s Note: The statements, opinions and data contained in all publications are solely those of the individual author(s) and contributor(s) and not of MDPI and/or the editor(s). MDPI and/or the editor(s) disclaim responsibility for any injury to people or property resulting from any ideas, methods, instructions or products referred to in the content.